

Compressor-Driven Metal Hydride Heat Pump System의 동작특성에 관한 연구

The Operating Characteristics of the Compressor-Driven Metal Hydride Heat Pump System

Jeong-Gun Park, Chan-Yeol Seo, a)Paul. S. Lee and Jai-Young Lee
Department of Materials Science and Engineering, Korea Advanced Institute of
Science and Technology, Kusong-dong 373-1, Yusong-gu, Taejon 305-701, South
Korea a)KLA Tencor, San Jose, California, U.S.A

Absatact

Metal hydride을 이용하는 냉방시스템은 다른 냉방시스템과 비교하여 환경 친화적이며 Clean technology라는 장점이 있다. 이러한 시스템 중에 최근에 많은 연구가 진행중인 Electric Compressor로 수소의 이동이 제어되는 Compressor-Driven Metal Hydride Heat Pump(CDMHHP)은 폐열원의 온도에 의해 제어되는 시스템에 비하여 cooling power가 크다는 장점과 함께 단속적인 냉방이 아닌 2개의 함금쌍으로도 연속적인 냉방이 가능하다는 장점이 있다. 본 연구에서는 이러한 CDMHHP system의 동작특성을 분석하기 위해서 2개의 반응관에 고용량과 solping 특성이 매우 우수한 $Zr_{0.9}Ti_{0.1}Cr_{0.55}Fe_{1.45}$ Laves phase metal hydride을 장입하여 시스템을 구성하고 cycle time, surrounding temperature, 장입 수소량, 수소이동량등의 동작조건을 최적화 한 결과 최대 cooling power가 251 kcal/kg-alloyh의 우수한 성능을 보였다.

Keywords: Metal hydride, CDMHHP, Compressor, Cooling power

1. Introduction

In recent years, various thermally driven solid sorption systems using different working hydride pairs (Metal Hydride Heat Pump, MHHP) have been investigated regarding their heating, cooling and heat transformation applications [1-4]. The goal of this investigation is to make them competitive with the conventional vapor compression systems and also with commercially available liquid sorption systems. For this, the cooling power must be increased. However conventional MHHP has some problems to be solved.

- i) In conventional MHHP is inefficient because of the discontinuous power output. Here the regenerator hydride as a heat-driven hydrogen compressor function is essential, but produces no cooling power.
- ii) The regenerator hydride must be heated up to high temperature (generally $DT > 150^{\circ}\text{C}$). So, the decrease of cycle time is limited.
- iii) Only 50-60% of reversible hydrogen can be used.

To obtain high power needed in environment and/or economical aspects, these problems must be solved. Recently, *Kim et al.*[5] and other authors [6-7] reported the experimental data on the compressor-driven metal hydride heat

pump. These studies indicate that the system has the potentiality to obtain more power because it did not need the regenerator hydride and as a result, the cycle time can be shortened drastically [5]. However the cooling power of about 200 kcal/kg-alloyh [5] is not so high compared with conventional MHHP system. It may be due to mismatching in selection of metal hydride for a given compressor properties. In this work, we selected a Zr-based metal hydride considering the properties of compressor, constructing a CDMHHP system, and investigated the operating characteristics of the system.

2. Compressor-Driven MHHP (CDMHHP) system

Figure. 1 shows the principle of the CDMHHP. Two reactors, filled with the same metal hydride, are connected to a compressor. Initially, one reactor is charged with hydrogen and the other is depleted. The charged reactor is cooled when hydrogen is desorbed and the depleted reactor is heated when hydrogen is compressed. Thereafter the process runs in the reversed direct. If the air from the indoor space is circulated over the cold reactor, the indoor space is cooled, during the outdoor air is blown over the hot reactor for rejecting heat of hydrogen absorption. An insulated

damper changes the direction of the air circulation alternately over the one reactor and over the other reactor. This heat pump can be used also as heating apparatus, if the heating period of the reactor is utilized. In the winter season, therefore warm air can be produced for heating the indoor space.

3. Design of tested reactors

Figure. 2 shows reactor pair, i.e. two fin-tube type heat exchangers. To enhance the effective thermal conductivity of the hydride powder bed, gasket type heat conducting matrices (Al alloy) with 0.1 mm in thickness have been installed. Consequently, the effective thermal conductivity is enhanced by over 7 W/mK. The tube for the reactor is 15 mm in diameter and 0.8 mm in wall thickness. To enhance the hydrogen transfer, stainless steel mesh filter is introduced in the center of the reactor tubes. The metal hydrides used are the Zr-Ti-Cr-Fe based AB_2 -type Laves phase alloy. The density of the hydride powder bed is about 4 g/cm^3 so that the porosity is about 53%. The weight of metal hydride filled in a reactor is 4.2 kg.

4. Experimental Setup

An oil-less type air-operating compressor (Haskell Co., USA) was chosen to avoid the problem of the oil vapor contamination (Figure 3). This compressor is cylindrical (piston type) model driven only by compressed air not by electric power. Its maximum compressing pressure and the minimum suction pressure are 20 atm and 0.5 atm respectively. The hydrogen flow rate can be controlled from 17 to 160 slm (standard liter per minute) by controlling the suction pressure. Figures. 4(a) and 4(b) show CDMHHP system from the different points of view. Two three-way valves operated automatically were installed to alternate the hydrogen flow direction. Pressure and temperature at various locations of the CDMHHP system were monitored by pressure transducers (Omega Co.) and K-type thermocouples and all connected to a scanning thermometer (Keithley Co.). A computer-based data acquisition system (GPIB interfacing card, PCLD card with a relay board) was used to read the signal output and to control the three-way valves.

5. Results and discussion

In selecting the metal hydride, the properties of the compressor (the theoretical maximum compressing pressure of 20 atm and the minimum suction

pressure of 0.5 atm. The hydrogen flow rate of 160 liter/min at 5 atm and 17 liter/min at 0.5 atm) must be considered. The metal hydride must have high hydrogen storage capacity, fast kinetics, low sloping and hysteresis, high hydride formation enthalpy basically. In addition, its plateau pressure at the heating period must be lower than the maximum compressing pressure of the compressor and its plateau pressure at the cooling period must be higher than the minimum suction pressure of the compressor. Also, to enhance the hydrogen flow rate, plateau pressure at the room temperature must be about 5 atm because the hydrogen flow rate is maximized at this hydrogen pressure. Considering all of these, $Zr_{0.9}Ti_{0.1}Cr_{0.55}Fe_{1.45}$ alloy [8], which showed good cyclic property [9] and fast hydrogen absorption/desorption rate compared with $LaNi_5$ type alloys, was selected for the CDMHHP system. As shown in Figure 5(a), the hydrogen storage capacity is 1.6 wt% and hydride formation enthalpy is 7 kcal/mol H_2 . In this CDMHHP system, the alloy can be cooled to 5 °C theoretically (Figure 5(b)). To obtain the maximum cooling power, it is important to optimize the operating parameters. The main operating parameters are initial hydrogen pressure, cycle time, surrounding temperature (room temp.) and airflow rate. Figures 6(a) and (b) show the temperature and pressure profiles at the typical operating conditions. It is found that the real operation

pressure of compressor in this system is between 1 atm and 18 atm, and the minimum cooling temperature is 11 °C at air flow rate of 4.5 m³/min. The effects of several parameters on the system performance are as follows.

5.1. Effect of the cycle time

As shown in Figure 7(a), the cooling power shows a maximum behavior. In general, the cooling power is described as a function of the amount of transferred hydrogen and the cycle frequency. As cycle time increases the amount of transferred hydrogen increases. However, the cycle frequency decreases. As shown in Figure 7(b) there is an optimum cycle time, which leads to the maximum output of the cooling power. In the experiment, the maximum output was obtained at the cycle time of 2.6 min.

5.2. Effect of the amount of charged hydrogen

The amount of charged hydrogen can be expressed as the initial hydrogen pressure. As the initial hydrogen pressure increases the amount of stored hydrogen increases. Therefore the cooling power also increases (Figure 8(a)). However, the initial hydrogen pressure over 7 atm causes to decrease the cooling power with limited maximum operating pressure of the compressor (Fig. 8(b)) and then with decreasing the amount of transferred hydrogen.

5.3. Effect of surrounding temperature

As the surrounding temperature increases the cooling power also increases (Figure 9(a)). Generally, in the cooling period, as the temperature of alloy decreases and the plateau pressure falls down. When the surrounding temperature is high, the difference between the desorption pressure and the bottom limit pressure of the compressor is large (Figure 9(b)). Therefore, the amount of transferred hydrogen has increased, which leads to increase the cooling power.

5.4. Effect of the airflow rate

As the airflow rate increases, the cooling power also increases (Figure 10(a)). However the cooling power is saturated at above $11\text{m}^3/\text{min}$. As shown in Figure 10(b), the rate-controlling step is the heat transfer on the surface of the reactor tube

by convection at the low airflow rate. As the airflow rate increases, the heat transfer on the surface has improved, but the heat conduction in the hydride bed stays almost the same. In the case, the total heat transfer is controlled by the heat conduction in the bed.

By controlling the operation parameters, the cooling power of $251\text{ kcal/kg-alloyh}$, was obtained. The optimized operating conditions are the cycle time of 2.6 min, the flow rate of $11\text{m}^3/\text{min}$, the initial

hydrogen pressure of 7 atm and operating temperature of $24\text{ }^\circ\text{C}$. The cooling power of this system is very high considering the cooling power of about $150\text{ kcal/kg-alloyh}$ [10] in a conventional heat pump system. Figure 11(a) and (b) show profiles of cooling power and temperature at the optimum operating conditions. From the above results, it can be found that the system performance such as minimum cooling temperature or maximum cooling power is dependent only on the related properties of metal hydride and compressor.

However, in these experiments, COP (coefficient of performance) of the system and the hydrogen flow rate could not measured because the oil-less type compressor, which was operated only by compressed air not electric power and which push the hydrogen discontinuously, was used. In this case, a mass flow controller (MFC) did not operate properly. To solve this problem and to evaluate the system performance exactly, an improved CDMHHP system is constructing now.

6. Conclusions

A Compressor-Driven Metal Hydride Heat Pump system was developed. The $\text{Zr}_{0.9}\text{Ti}_{0.1}\text{Cr}_{0.55}\text{Fe}_{1.45}$ Laves phase alloy for the system was selected as a suitable metal hydride for the given compressor to operate in a pressure range from 1 atm to

18 atm. The hydrogen storage capacity of the alloy is 1.6 wt%, the hydride formation enthalpy is 7 kcal/mol H₂ and the plateau pressure at 30 °C is 5 atm. The optimum operating conditions are the cycle time of 2.6 min, the flow rate of 11m³/min, the initial hydrogen pressure of 7 atm and the surrounding temperature of 24 °C. At these conditions, the maximum cooling power of this system is 251 kcal/kg-alloyh.

Reference

- [1] E. Tucher, P. Weinzierl and O. J. Eder, Dynamic characteristics of single- and double-hydride bed devices. *J. Less-Common Metals* 95 (1983) 171-179
- [2] H. Bjurstrom, Y. Komazaki and S. Suda, The dynamics of hydrogen transfer in a metal hydride heat pump. *J. Less-Common Metals* 131 (1987) 225-234
- [3] M. Nagel, M. Komazaki and S. Suda, Dynamic behavior of paired metal hydrides. *J. Less-Common Metals* 120 (1986) 45-53
- [4] M. Gambini, Metal hydride energy systems performance evaluation. Part A: Dynamic analysis model of heat and mass transfer. *Int. J. Hydrogen Energy* 19 (1994) 67-80
- [5] Kim. K.J., K.T. Feldman, Jr. G. Lloyd and A. Razani. *Applied Thermal Engineering* 1997. 17(6) 551-560
- [6] Wolf. S. Proceedings of the 10th Intersociety Energy Conversion Engineering Conference (IECEC), 1975, paper 759196, 1348-1351
- [7] McClaine, A.W. U.S.Patent 4,039,023 (1977)
- [8] J.Y.Lee, J.M.Park, U.S. Patent 5,028,389 (1991)
- [9] H. H. Lee, J. Y. Lee, The Intrinsic degradation behaviors of the Laves phase Zr_{0.9}Ti_{0.1}Cr_{0.9}Fe_{1.1} upon the temperature-induced hydrogen absorption-desorption cycling, *J. of Alloys and Compounds*, 202 (1993) 23
- [10] S. G. Lee, Y. K. Kim, and J. Y. Lee, Operating characteristics of metal hydride heat pump using Zr-based Laves phases, *Int. J. of Hydrogen Energy*, vol.20 , No.1 (1995) 77-85

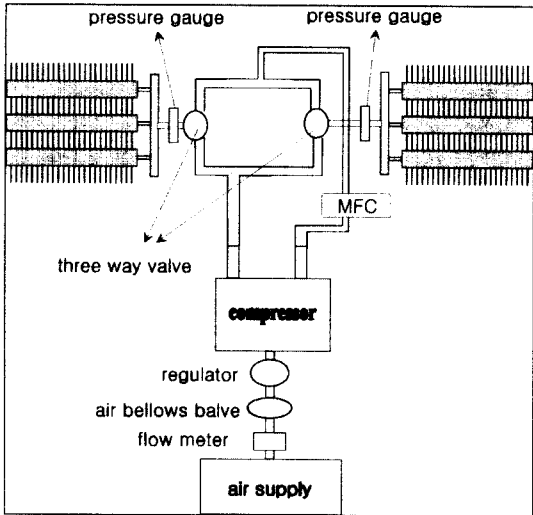


Figure 1. A schematic diagram of CDMHHP system

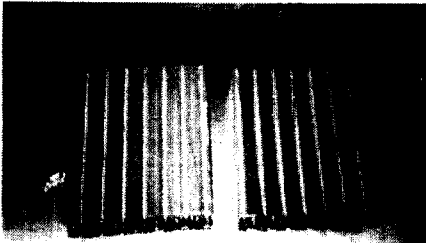


Figure 2. A photo of reactors

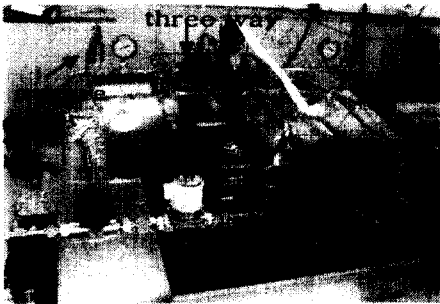


Figure 3. A photo of oilless type compressor

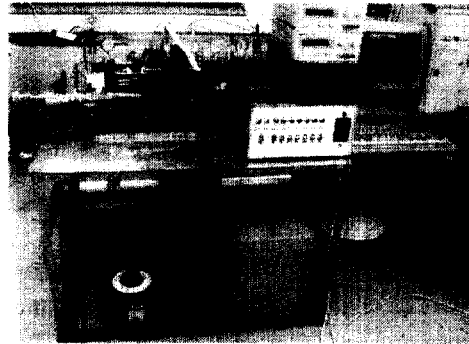


Figure 4(a). Rear view of the CDMHHP

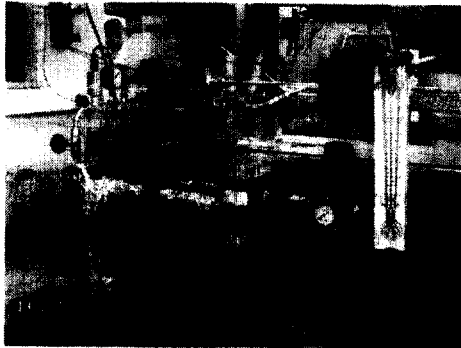


Figure 4(b). Side view of the CDMHHP

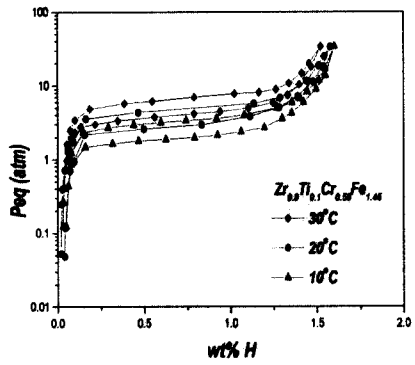


Figure 5(a). P-C-T curves of $Zr_{0.9}Ti_{0.1}Cr_{0.55}Fe_{1.45}$ at various temperature

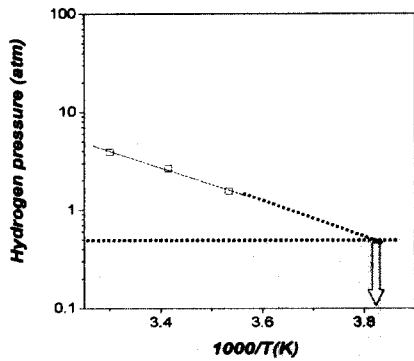
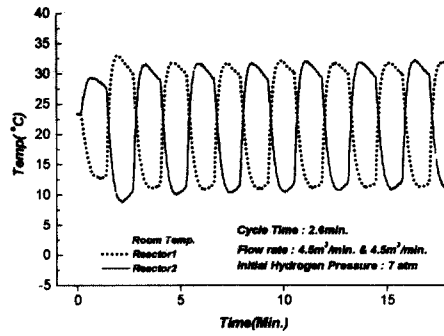
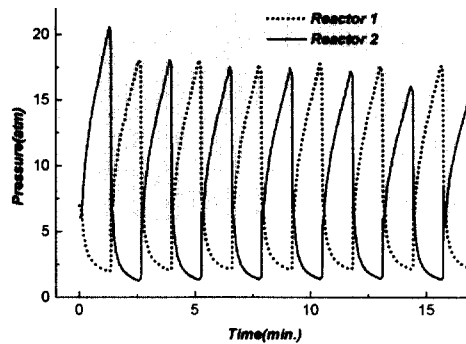


Figure 5(b). van't Hoff plot of $Zr_{0.9}Ti_{0.1}Cr_{0.55}Fe_{1.45}$



(a)



(b)

Figure 6. Pressure (a) and temperature (b) profiles in various reactors under the typical operation conditions

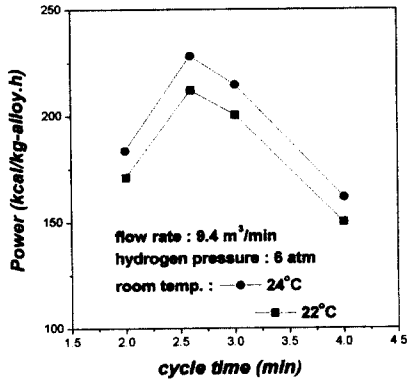


Figure 7(a). Cooling power as a function of cycle time

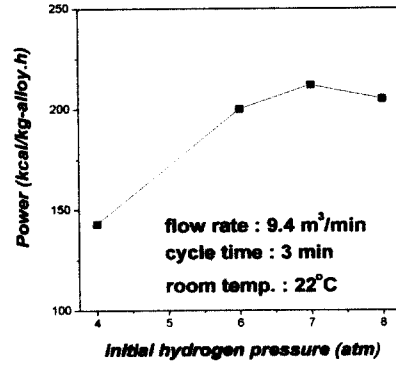


Figure 8(a). Cooling power as a function of initial hydrogen pressure

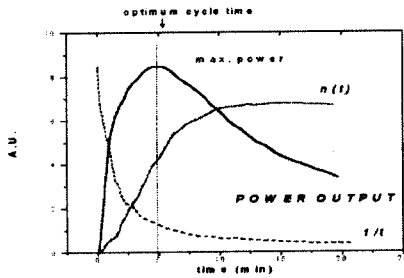


Figure 7(b) Schematic diagram of cooling power as a function of cycle time. $n(t)$ means the amount of transferred hydrogen. $f(t)$ means the cyclic frequency

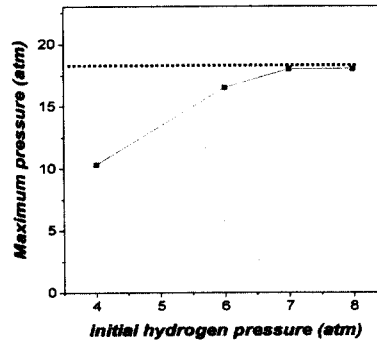


Figure 8(b). Maximum pressure of system as a function of initial hydrogen pressure

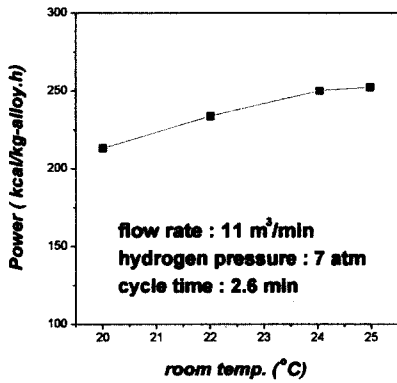


Figure 9(a). Cooling power as a function of surrounding temperature

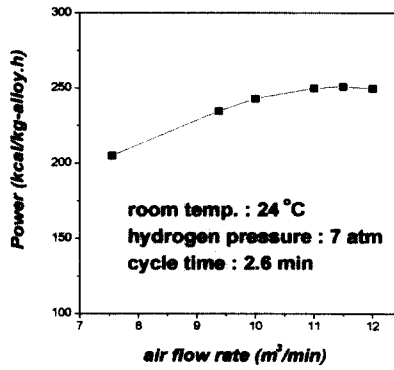


Figure 10(a). Cooling power as a function of air flow rate

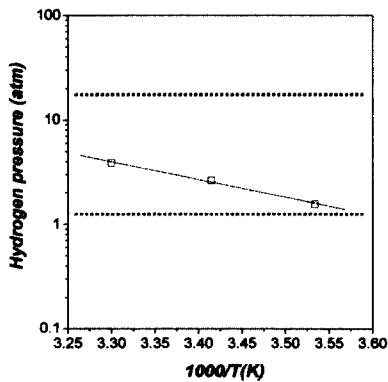


Figure 9(b). van't Hoff plot of $Zr_{0.9}Ti_{0.1}Cr_{0.55}Fe_{1.45}$ (desorption pressure)

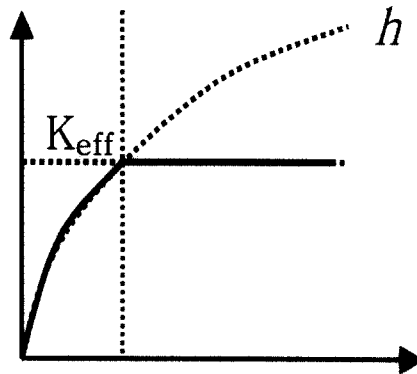
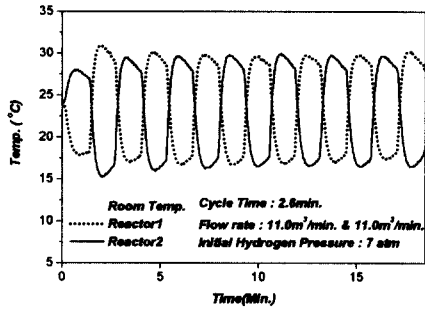
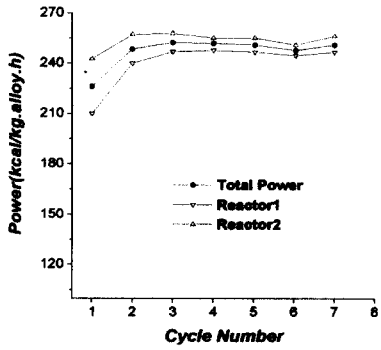


Figure 10(b). Schematic diagram of the rate controlled step as a function of the air flow rate



(a)



(b)

Figure 11. Temperature (a) and cooling power (b) profiles in various reactors at optimum operation condition